Subpicosecond Transient Dynamics in Gold Nanoparticles Encapsulated by a Fluorophore-Terminated Monolayer

Tao Gu,[†] Tong Ye,[‡] John D. Simon,[‡] James K. Whitesell,[†] and Marye Anne Fox*[,†]

Department of Chemistry, North Carolina State University, Raleigh, North Carolina 27695-8204, and Duke University, Durham, North Carolina 27708-0349

Received: August 30, 2002; In Final Form: December 19, 2002

Gold nanoparticles (2.2 nm) protected by a densely packed monolayer of 9-(9-fluorenyl)-nonane-1-thiol (MPC-b) or a mixed monolayer of 9-(9-fluorenyl)-alkane-1-thiol with nonane-1-thiol (MPC-c and MPC-d) were studied by transient spectroscopy upon 305 nm excitation with subpicosecond laser pulses. Electronic relaxation of the gold core took place through a fast electron−phonon interaction within 2.0 ps, followed by a slow phonon−phonon interaction over a period longer than 15 ps. Electronic coupling of the excited fluorenyl groups with the gold core in these composite clusters affected the observed gold electron relaxation dynamics, likely by adding an excitation path for gold electrons by working as a sensitizer. The efficiency of energy transfer from the excited fluorene to the gold particles was affected by surface composition, with the ratio of the fast decay component to the slow decay component decreasing upon increasing the fraction of fluorenyl groups present at the surface. Thus, energy transfer from the excited fluorene to the gold nanocore is a dominant relaxation mode for the fluorene excitons in chromophore-labeled monolayer protected gold clusters, taking place with a rate constant k_{EN} estimated to be greater than 10^{12} s^{-1}.

Introduction

Nanoparticles exhibit unique electronic, magnetic, and optical properties because of their small size and large surface-to-volume ratio.[1−3] Time resolution of transients produced by pulse excitation from an ultrafast laser permits the study of charge carrier dynamics in both metallic clusters and nanoparticulate composites. Relaxation of electrons in such composites from a non-Fermi distribution and subsequent thermalization through electron−electron, electron−phonon, and phonon−phonon interactions have been investigated in different metal nanoparticle sizes and surrounding environments (organic or inorganic matrix, polar, or nonpolar solvents, etc.). These studies show that electron−phonon relaxation rates in metallic nanoparticles are generally independent of their size or shape.[4]

On the other hand, relaxation dynamics do depend on the local environment of the excited species. For example, Zhang et al. reported electron−phonon interaction relaxation times varying from 7 ps in water to 3.5 ps in cyclohexane for 18 nm Pt particles.[5] Bigot et al. reported that the electron−phonon relaxation increased from 0.77 ps in an alumina matrix to 1.4 ps in a glass matrix.[6] El-Sayed et al. reported that the electron−phonon relaxation time is slower by a factor 2 for the gold nanoparticles embedded in $MgSO_4$ powder than in solution.[7] Furthermore, adding solvent to the particles embedded in the powder caused a further decrease from 10 to 5 ps. These results indicate that observed electronic relaxation times in these gold nanoparticles are sensitive to surface structure, depending on the chemical nature and/or physical phase (solid vs solution) of the encapsulant.[7]

We have reported previously photoinduced energy transfer from an excited fluorenyl singlet to the gold nanocore in the 9-(9-fluorenyl)-alkane-1-thiolate monolayer-protected gold clusters (MPCs),[8a] Scheme 1. High loading of a fluorene-containing thiol on the gold clusters was enabled by the enthalpic gain associated with dense packing of the methylene chains, producing a fluorene-terminated shell covering the gold clusters. With nanosecond flash photolysis, we demonstrated that a gold nanocore interacts strongly with a bound excited fluorenyl singlet, causing quenching of fluorescence and suppressing intersystem crossing from the excited singlet to the triplet state. In this paper, ultrafast spectroscopy was used to probe further the nature of this electronic coupling between the excited

SCHEME 1: Partial Structures of Monolayer-Protected Clusters, Capped by (a) Nonane-1-thiol, (b) 9-(9-Fluorenyl)-nonane-1-thiol, (c) Mixed Monolayer of 9-(9-Fluorenyl)-dodecane-1-thiol and Nonane-1-thiol, and (d) Mixed Monolayer of 9-(9-Fluorenyl)-nonane-1-thiol and Nonane-1-thiol

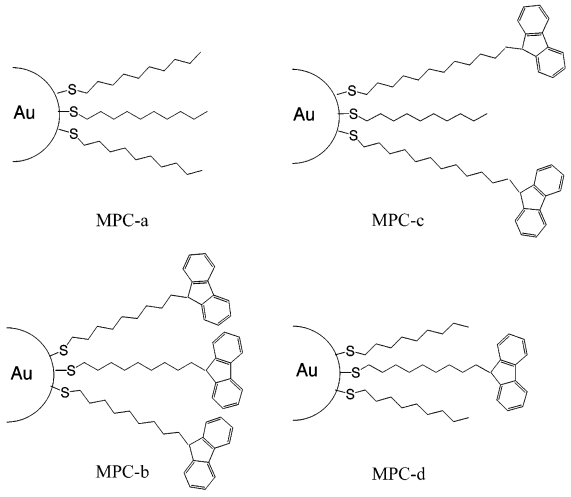

* Corresponding author.
[†] North Carolina State University.
[‡] Duke University.

10.1021/jp026884l CCC: $25.00
Published on Web 01/29/2003

SCHEME 2: Structures of 9-(9-Fluorenyl)-nonane-1-thiol (1) and 9-(9-Fluorenyl)-dodecane-1-thiol (2)

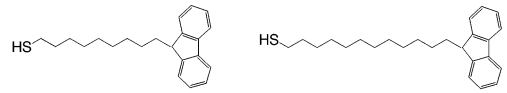

1 **2**

fluorene and the gold core. Our approach here involves monitoring electronic relaxation dynamics of the metal d band.

Experimental Section

All reagents and solvents were reagent grade and were used without further purification. NMR spectra were recorded on a Varian 300 or 400 MHz instrument with solvent peaks as reference. Absorption spectra were recorded on a Shimadzu PC-3101PC instrument.

Transmission electron microscopic (TEM) studies were performed with a Hitachi HD-2000 STEM (200 keV) spectrometer. TEM samples were prepared by drop casting a solution of nanoparticles in toluene, typically at a concentration of 1 mg/mL, onto a grid with 50 or 150 nm silicon nitride membrane windows. Phase-contrast TEM micrographs were typically taken at three different spots of the grids with 500−2000 K magnification. Particle size analysis was then performed by digitizing the micrographs with Scion image software (available at www.scioncorp.com), from which the histograms of the particle size distribution was generated. Twin or particle aggregates were removed manually prior to size measurements.

9-(9-Fluorenyl)-nonane-1-bromide was prepared using a modification of the Cedheim and Eberson procedure.[8b] The corresponding thiol was prepared in high yield from the bromide by a previously reported displacement reaction.[8c]

Nonane-1-thiolate gold clusters (MPC-a) were prepared by Murray's procedure,[8d] in which $NaBH_4$ reduction is conducted at room temperature through fast addition to a solution in which the mole ratio of thiol/$HAuCl_4 \cdot 3H_2O$/tetraoctylammonium bromide/$NaBH_4$ is 2:1:2.5:10.

The fluorene-labeled MPCs were prepared by place-exchanges of the initial nonane-1-thiolate ligands (on $Au_{323}(SC_9H_{19})_{113}$) with 9-(9-fluorenyl)-alkane-1-thiolate.[8a] A toluene solution of MPC-a with **1** or **2** (Scheme 2) was stirred at room temperature for 3 days. Solvent was then removed under vacuum, and the resulting precipitate was washed copiously with ethanol and acetone to remove any unreacted **1** or **2** ligands and displaced nonane-1-thiol before being collected via filtration. The absence of sharp peaks in the ^{1}H NMR spectra demonstrated the removal of all nonligated thiols. A series of fluorene-labeled MPCs were prepared with different alkane chain length and different feeding ratio of nonane-1-thiol with **1** or **2** (see Table 1).

Tunable femtosecond laser pulses were generated from a commercial system with a 1 kHz repetition rate, regeneratively amplified, titanium−sapphire laser (Spectra Physics). The output pulses of the regenerative amplifier were generally 120 fs (fwhm) and 0.8 mJ/pulse at 800 nm. These pulses were used to pump an optical parametric amplifier (OPA, Spectra Physics). The pulses from the OPA were 220 fs (fwhm) and approximately 3 μJ/pulse and were split into pump and probe pulses for performing degenerate transient absorption measurements.

The pump and probe excitation pulses traveled different paths and were focused and recombined at the sample. A stepper-motor-driven translation stage enabled the time of arrival of the pump and probe pulses at the sample to be varied; the minimum step size corresponded to a delay time of 17 fs. The probe pulses were split into two so that intensity could be monitored before and after passing through the sample, and subsequently the time-dependence of the transient absorption signal could be calculated.

The intensity was measured using a photodiode (UDT UDT-020UV) interfaced to a computer-controlled lock-in amplifier (Stanford Research Systems SR850). All experiments were performed with the relative polarization of the pump and probe beam set at the magic angle. Data were recorded using time increments of 850, 50, and 17 fs. The traces reported herein represent a combination of time scales using all three step sizes.

For degenerate pump−probe experiments, the concentration of all the sample solutions was adjusted to give an absorbance of 0.50 in a 1 mm cuvette at the excitation wavelength. Sample solutions were run through a 1 mm flow cell and the absorptions of the solutions did not change over the course of an experiment.

TABLE 1: Composition of MPCs

sample name	feed ratio: cluster ligand/thiol[a]	percentage of ligands exchanged[b]	composition[c]
MPC-a			$Au_{323}(C_9H_{19}S)_{113}$
MPC-b	1/2.22	100	$Au_{323}(C_{22}H_{28}S)_{113}$
MPC-c	1/1.965	81.49	$Au_{323}(C_{25}H_{34}S)_{92}(C_9H_{19}S)_{21}$
MPC-d	1/0.416	48.26	$Au_{323}(C_{22}H_{28}S)_{54}(C_9H_{19}S)_{59}$

[a] Feed ratio of nonane-1-thiolate ligands on $Au_{323}(SC_9H_{19})_{113}$ to 9-(9-fluorenyl)-alkane-1-thiol **1** or **2**. [b] The percentage of the initial nonane-1-thiolate ligands (on $Au_{323}(SC_9H_{19})_{113}$) exchanged by 9-(9-fluorenyl)-alkane-1 thiolate ligands (**1** or **2**) was established by ^{1}H NMR. [c] The average composition of nonane-1-thiolate MPC was established by TEM and elemental analysis with the assumption that the average MPC core has a closed-shell structure and a roughly spherical shape. ^{1}H NMR was then used to measure the ratio of nonexchanged alkane-1-thiolate ligands to exchanged 9-(9-fluorenyl)-alkane-1-thiolate ligands. The ratio was converted into numbers of exchanged ligands based on the average composition of nonane-1-thiolate MPC. A detailed calculation has been discussed in a previous paper.[8a]

Results

The average core diameter of nonane-1-thiolate MPCs (MPC-a) was established by TEM (Figure 1) and the organic fraction of surface coverage was calculated from elemental analysis. This calculation assumed that the average MPCs core would have a closed-shell structure and a roughly spherical shape. A densely packed nonane-1-thiolate MPC with an average core diameter of 2.2 nm (standard deviation 0.7 nm) would give an average formula of $Au_{323}(S(CH_2)_9H)_{113}$.[8a] The fraction of fluorophores loaded onto the clusters by place-exchange was established by ^{1}H NMR.[8a] The ^{1}H NMR spectra of all fluorenyl-capped MPCs were characteristically broadened relative to those of free 9-(9-fluorenyl)-alkane-1 thiols homogeneously dispersed in solution. The absence of sharp peaks in the ^{1}H NMR spectra demonstrated the removal of all nonligated thiols.

In the steady-state absorption spectra of the gold clusters capped with 9-(9-fluorenyl)-nonane-1-thiol (MPC-b), Figure 2, there is no distinct surface plasmon band present, but rather strong trailing absorption starting at 1.7 eV (750 nm) and continuing into the long wavelength ultraviolet.[9] The absence of a plasmon band in small metallic particles has been attributed to quantum-size effects: evolution of plasmon absorption as a prominent band is seen only for particles of diameters > 5 nm.[9,10] The average nanoparticle size obtained here (2.2 nm) is thus consistent with the absence of a surface plasmon band. The absorption in the 250−350 nm region shows three distinct absorption bands (266, 290, and 302 nm), characteristic of

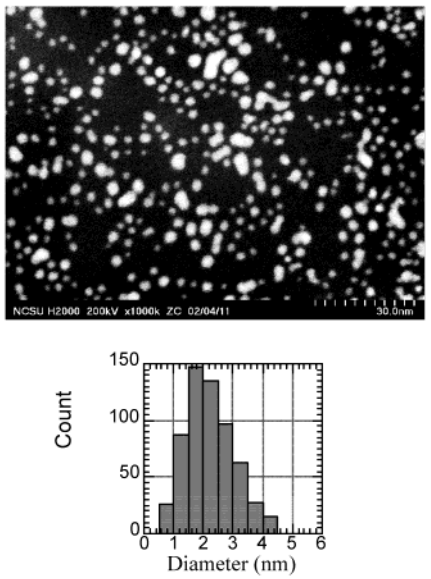

Figure 1. (a) TEM micrograph of dropcast film of nonane-1-thiolate-protected Au clusters (MPC-a). (b) Size histogram for TEM micrograph in Figure 1a. The mean size is 2.2 nm and the standard deviation is 0.7 nm.

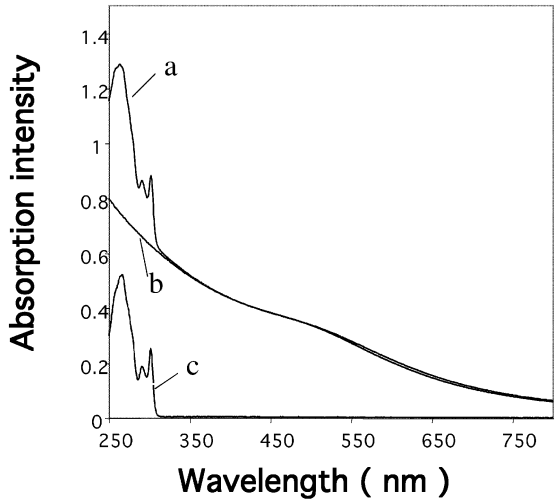

Figure 2. Absorption spectra in dichloromethane of (a) 9-(9-fluorenyl)-nonane-1 thiolate MPCs (MPC-b), (b) nonane-1-thiolate MPCs (MPC-a), (c) 9-(9-fluorenyl)-nonane-1 thiol **1** (2.2×10^{-5} M).

fluorenyl groups. The MPC-b shows no additional absorption peaks upon fluorenyl groups chemically binding to the surface of the gold clusters. Instead, the spectrum is a simple superimposition of a fluorene absorption on that of MPC-a.

In the flash experiments, absorption spectra of all the samples were measured before and after the laser pulses. No changes in absorption shape or maxima were observed, although intensity increased slightly, presumably because the samples became concentrated somewhat during the experiment. Laser-induced shape changes of the nanoparticles have been reported at higher incident energies, including fusion, fragmentation, shape changes (nanorods changing into nanodots), etc.[11,12] The visible region of each absorption spectrum was closely monitored in order to discern any shape transformation affecting the plasmon absorption bands,[12] which would show obvious change if the nanoparticle were to participate in any morphological change during flash excitation. Unchanged absorption spectra therefore indicate the absence of the morphological change in the nonane-1-thiol- or 9-(9-fluorenyl)-alkane-1-thiol-protected gold nanoparticles (MPC-a, b, c, and d) during the laser pulse.

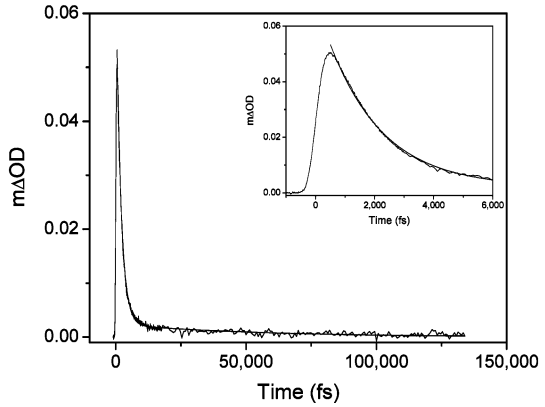

Figure 3. Dynamics for relaxation of nonane-1-thiolate MPCs (MPC-a). The smooth line is a fit with lifetimes of 1.8 and 26 ps. Inset: expansion of the short time scale.

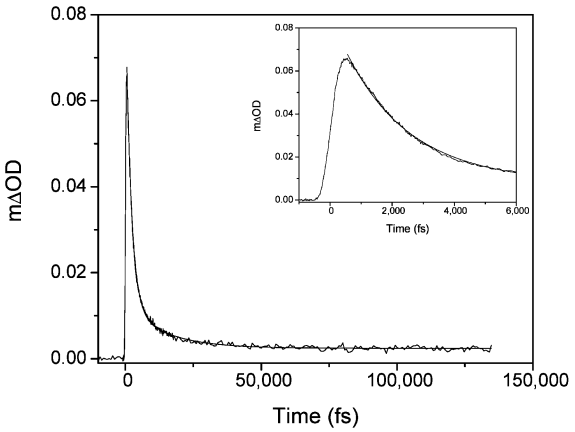

Figure 4. Dynamics for relaxation of 9-(9-fluorenyl)-nonane-1 thiolate MPCs (MPC-b). The smooth line is a fit with lifetimes of 2.0 and 14 ps. Inset: expansion of the short time scale.

Figure 3 shows the transient absorption at 400 nm obtained upon flash excitation of MPC-a. The transient was obtained at room temperature with 200 fs pump and probe pulses centered at 305 and 400 nm. Following the appearance of an instantaneous absorption, the transient decays by biexponential kinetics with time constants of 1.8 and 26 ps. The ratio of the amplitude of the fast component to the slow component is found to be 28.

For MPC-b, photoexcitation at 305 nm by 200 fs laser pulses leads to the absorption changes shown in Figure 4. The decay dynamics of this transient absorption is also biexponential with a lifetime of the fast component found to be 2.0 ps; the slow component is found to be 14 ps. The amplitude ratio of these two components is found to be 7. That is, a larger fraction of the observed decay proceeds through the slower channel.

To study the effect of a fluorenyl monolayer encapsulating the gold nanocore in a chromophore-labeled MPC on electronic relaxation dynamics, we also prepared a solution of MPC-a with unattached **1**, which has absorption identical to that of the MPC-b, and was defined as Match-b′.

The thiolates bound to Au atoms lying at the intersection of two flat faces are denoted as edge sites and those thiolates bound to Au atoms lying at the intersection of three flat faces are denoted as vertice sites. These sites have been proved to be the most easily exchanged sites.[12b] It appears that about 4 most readily exchangeable sites are available on 2.1 nm diameter $Au_{314}(RS)_{108}$.[12b] A solution of MPC-a and unattached **1** (Match-b′, structure see Scheme 3b), which has absorption identical to that of MPC-b, is prepared just before the dynamics experiment. Even though a small amount of 9-(9-fluorenyl)-alkane-1-thiol

SCHEME 3: Proposed Pathways with Which the Excited Fluorene undergoes Deactivation. (a) The Excited Fluorene in Solution of MPCs Capped with 9-(9-Fluorenyl)-Nonane-1-Thiol (MPC-b) Undergoes Energy Transfer. (b) The Excited Fluorene in Solution of the Nonane-1-thiolate MPCs and Unattached 9-(9-Fluorenyl)-nonane-1-thiol (Match-b′), Which Is Optically Matched to MPC-b, Undergoes Energy Transfer. (c) The Excited Fluorene in Match-b′ Solution Undergoes Intersystem Crossing

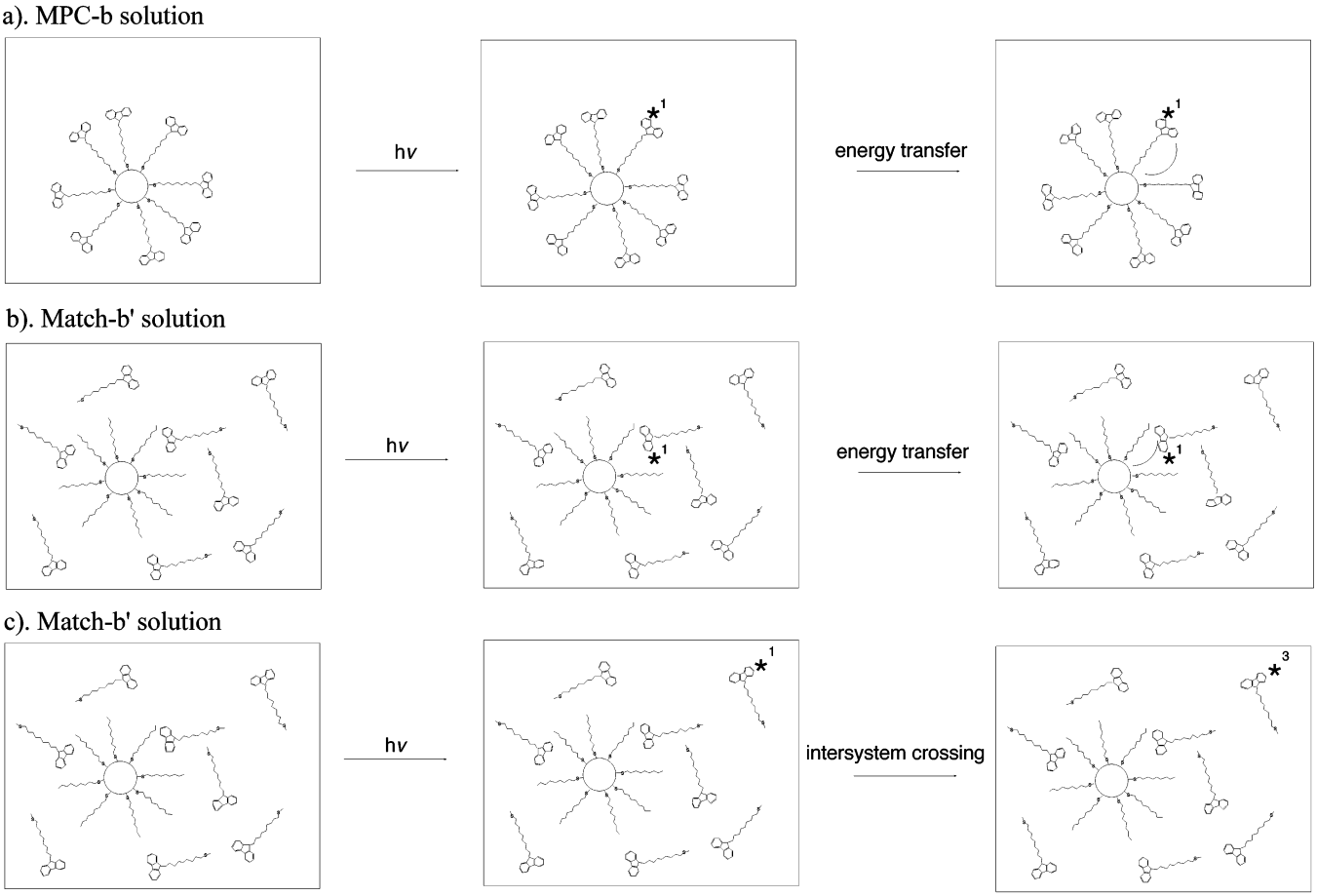

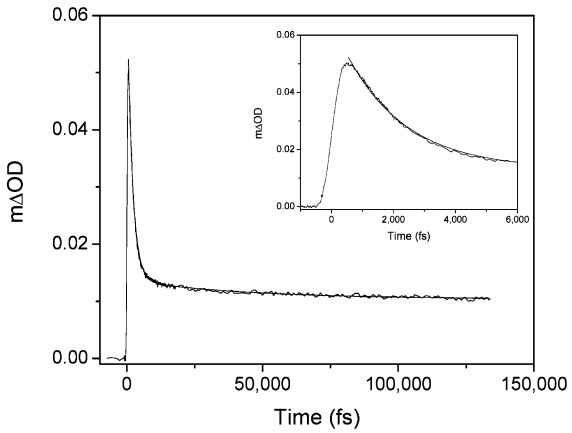

Figure 5. Dynamics for the relaxation of Match-b′ solution. The smooth line is a fit with lifetimes of 1.9 and 44 ps. Inset: expansion of the short time scale.

exchanged with the nonane-1-thiolate ligands at the readily-exchanging sites on gold core, we believe that most of the fluorenyl groups are unattached to the gold surface in the optically matched solution during the flash experiments.

Photoexcitation with 305 nm with a 200 fs laser pulse for Match-b′ leads to the absorption changes shown in Figure 5. The decay dynamics of the transient absorption is biexponential, similar to that of the MPC-a. The lifetimes of the fast and slow components of this transient decay were found to be 1.9 and 44 ps, respectively, in a ratio of 15. The obvious difference between this solution and MPC-b is that the transients exhibit residual absorption of roughly 16% of the total amplitude for probe delay times until 140 ps (the time limit of our experiment).

Transient decay was also measured for gold nanoparticles capped with a mixed monolayer of 9-(9-fluorenyl)-alkane-1-thiol with nonane-1-thiol (MPC-c and MPC-d), and the corresponding optically matched solution of MPC-a with unattached **1** or **2** (Match-c′ and Match-d′). Analyzing the transient dynamics results of different samples, we observed the following general features.

1. The MPC in which fluorenyl groups are bound to the cluster surface (MPC-b, c, and d) and the corresponding optically matched solution (Match-b′, c′, and d′) show similar electronic decay dynamics as in MPC-a. The observed transients decayed by a biexponential model with a short time scale of ∼2.0 ps and a longer one, typically ∼15 ps.

2. The residual absorption fraction in fluorenyl-capped gold clusters (MPC-b, c, and d) was smaller than that in the corresponding optically matched solution (Match-b′, c′, and d′).

3. The higher the fluorene percentage present in the capping monolayer of the MPCs, the larger the fractional residual absorption.

4. The ratio of the fast component to the slow component decreased in both fluorenyl-capped gold clusters (MPC-b, c, and d) and the corresponding optically matched solution (Match-b′, c′, and d′).

5. The ratios of the fast component to the slow component in fluorenyl-capped gold clusters (MPC-b, c, and d) were smaller than that in the optically matched solution (Match-b′, c′, and d′).

Discussion

Ultrafast dynamics of hot electrons in thin metal films have received much attention.[13a−e] Ultrafast excitation may produce a nonequilibrium distribution of electrons in the lattice of the films or clusters.[13f] Energy is redistributed among the electrons through electron−electron interactions, producing a hot Fermi distribution with temperature T_e. Internal thermalization of electrons in thin gold film was found to take place within several hundred femtoseconds.[13h] After electrons are thermalized, they lose their energy further by depositing energy into the lattice. The thermalization of an electronic gas takes place through electron−phonon coupling interactions, characterized by an exchange of energy at a rate proportional to $T_l - T_e$, through a process which has been measured to require several picoseconds for bulk gold. As the electron gas cools, it heats the lattice. This remaining thermal energy is lost to the surrounding medium through phonon relaxation processes.[13] Time evolution of the energies in the electrons system and phonon system is given by the coupled differential equations.[13g−j]

$$C_e(T_e)\partial T_e/\partial t = \nabla(\kappa \nabla T_e) - G(T_e - T_l) + P(x,t) \quad (1a)$$

$$C_l \partial T_l/\partial t = -G(T_l - T_e) \quad (1b)$$

where T_e and T_l are the electron and lattice temperatures, $C_e(T_e)$ is the temperature-dependent electronic heat capacity, C_l is the lattice heat capacity, κ is the thermal conductivity, G is the electron−phonon coupling constant, and $P(x,t)$ is the energy density per unit time absorbed from the incident laser beam.

Most of the literature[4−7,14−17] reported on electron relaxation dynamics in gold nanoparticles describes transients probed at 530 nm, which is the absorption maximum for the gold surface plasmon band. The transient signal at this probe wavelength was bleached and the plasmon bleaching recovery dynamics were observed. Usually, recovery from bleaching of the plasmon band took place with relaxation times of several to several hundred picoseconds. For example, Perner et al. reported relaxation times of 4 and 200 ps for 30 nm gold particles embedded in a sol−gel matrix.[14,15] Inouye et al. reported decay times of 2.8 and 120 ps for 7.6 nm gold nanoparticles in a SiO_2 glass matrix.[16] The fast decay was assigned to electron−phonon interactions and the slow decay to phonon−phonon interactions. The somewhat different time constants found for gold particles prepared in different labs might be due to different surface properties of the samples prepared, as suggested by the observed dependence of the relaxation time constant on surface composition, solvent, or chemical composition of the imbedded matrix.[5]

In flash photolysis experiments, a 305 nm laser pulse was used to excite the sample, and the transient absorption was probed at 400 nm. An excited fluorenyl singlet is generated at 305 nm. For Au, this same wavelength predominantly populates a 5d → 6sp interband transition; i.e., electrons are promoted from the filled 5d band to empty states above the Fermi level in the 6sp band.[18−20] The energy deposited by the pump laser is rapidly equilibrated among all the conduction band electrons by e−e scattering[21−25] on a time scale shorter than our time resolution. The further equilibration of the hot electrons takes place through external thermalization with the lattice by electron−phonon scattering and phonon−phonon relaxation. Fast electron−phonon relaxation requires about 2.0 ps and slow phonon−phonon relaxation requires about 26 ps in a nonane-1-thiolate MPC (MPC-a). These absorption decay dynamics are similar to those observed in the bleached plasmon band recovery, when a dodecane-1-thiolate MPC is pumped at 380 nm and probed at 530 nm. El-Sayed et al. reported that dodecane-1-thiolate MPCs with an average particle size of 1.9, 2.6, or 3.2 nm showed electron−phonon scattering over about 2−3 ps and phonon−phonon relaxation over periods longer than 50 ps.[17] Similar electron relaxation dynamics in fluorenyl groups chemically bound to the gold nanocluster system (MPC-b, Figure 4) and in an optically matched solution of nonane-1-thiolate MPCs with unattached 9-(9-fluorenyl)-nonane-1-thiol (Match-b′, Figure 5) also showed fast and slow decay components.

In MPC-b, residual absorption after electron relaxation over 140 ps constitutes less than 3% of the total amplitude. However, the residual absorption is more than 16% of the total amplitude in Match-b′, with most of the residual absorption being assigned to a fluorene triplet−triplet absorption. The disappearance of the expected triplet−triplet absorption in MPC-b implicates energy transfer from an excited fluorenyl singlet to the gold nanocore through an efficient relaxation channel, as we have inferred from early nanosecond flash photolysis studies.[8a] The short-lived transient decays of MPC-a and MPC-b are very similar, as judged by the instantaneous absorption rise correlated with a fast decay. Even though energy transfer from the excited fluorenyl group to gold was too fast to be observed directly, we conclude that this process must take place in less than 1 ps. That is, the energy transfer rate constant k_{EN} must be faster than 10^{12} s^{-1}. Otherwise, gold electron relaxation dynamics would show substantial difference over the shorter time range between MPC-a and MPC-b.

In a solution of unattached **1** and nonane-1-thiolate MPCs, the fluorenyl groups are homogeneously and freely dispersed in solution. Some of the fluorene molecules were very close to the gold particles, such that excited-state energy transfer was completed with the observed gold electron relaxation dynamics (Scheme 3b). Many of the fluorenyl groups located far from the gold particles gave no energy transfer, so that the excited fluorenyl singlet intersystem crossing to the triplet took place instead during the experiment's 140 ps time limit (Scheme 3c). The fluorene triplet−triplet absorption contributed significantly to the residual absorption observed by ultrafast decay dynamics. This is why the residual signal in the optically matched solution (Match-b′, c′, and d′) was larger than that observed for the fluorenyl-capped gold clusters (MPC-b, c, and d).

In Table 2 is shown evidence that the intensities of the residual absorption in the fluorenyl-capped MPCs (MPC-b, c, and d) and the corresponding optically matched solution (Match-b′, c′, and d′) vary with the percentage fluorenyl groups present at the periphery of the MPCs. In the MPC-b, the fluorenyl groups are packed densely on the gold core. All the excited fluorene exhibited energy transfer interaction with a gold nanocore via a distance-dependent energy transfer mechanism (Scheme 3a). In the corresponding optically matched solution Match-b′, small fractions of excited fluorenyl singlets participated in energy transfer to the gold core. Large fractions undergo intersystem crossing to the triplet. The residual from covalently capped 9-(9-fluorenyl)-nonane-1-thiolate MPCs (MPC-b) compared with the optically matched homogeneous solution (Match-b′) increased from 2.8% to 16%. Similarly, the residual for MPC-d compared with the optically matched solution (Match-d′) were very low, 0.8% and 1.5%, respectively. Thus, the higher the fluorene percentage in the encapsulate layer, the larger the

TABLE 2: Transient Dynamics for Nonane-1-thiolate MPCs (MPC-a), Fluorenyl-Capped MPCs (MPC-b, c, and d), and the Optically Matched Solutions of Nonane-1-thiolate MPCs and Unattached 1 or 2 (Match-b′, c′, and d′)

sample name	lifetime of fast component (ps)	lifetime of slow component (ps)	ratio of fast component to slow component	residual absorption (after 140 ps) to total absorption
MPC-a	1.8 ± 0.0	26.3 ± 4.0	28.0	0.7%
MPC-b	2.0 ± 0.0	14.2 ± 0.7	7.0	2.8%
Match-b′ [a]	1.9 ± 0.0	44.8 ± 5.3	15.0	16%
MPC-c	1.8 ± 0.0	14.8 ± 0.5	5.8	1.7%
Match-c′ [a]	1.8 ± 0.0	15.2 ± 1.0	10.9	6.9%
MPC-d	1.8 ± 0.0	13.3 ± 0.6	9.8	0.8%
Match-d′ [a]	1.8 ± 0.0	14.1 ± 1.1	10.9	1.5%

[a] Match-b′ is a solution of MPC-a and unattached **1**, which has identical absorption to MPC-b (with the same number of unattached **1** and gold clusters) and is prepared just before the dynamics experiment (structure see Scheme 3b). Match-c′ and Match-d′ have a similar definition.

difference in residual absorption between the fluorenyl-capped MPCs and the corresponding optically matched solution.

The nonane-1-thiolate MPCs (MPC-a) and the fluorenyl-capped MPCs (MPC-b, c, and d) all possessed an alkane chain protective layer. In the fluorene-labeled MPCs, the periphery-bound fluorenes could be excited at 305 nm, and the energy transfer to the gold nanocore was found to affect the gold electron relaxation dynamics, possibly by adding sensitization as an additional reaction path. The amplitude ratio of the fast component to the slow component of about 28 in nonane-1-thiolate MPCs (MPC-a) decreased to about 7 in 9-(9-fluorenyl)-nonane-1-thiolate MPCs (MPC-b) and to 15 in the optically matched solution of the nonane-1-thiolate MPCs with unattached 9-(9-fluorenyl)-nonane-1-thiol (Match-b′). El-Sayed reported that the relative contribution of the slow component in 30 nm gold nanoparticles became three times larger at higher laser intensities (laser pulse intensity from 20 μJ to 120 μJ) and that the lifetime of the fast component increased at higher intensity.[17] Thus, energy transfer from the excited fluorenyl group produced the same effects as did higher laser intensity. Although photoinduced energy transfer was not fast enough to change the electron relaxation lifetime appreciably, the ratio of the fast component to the slow component was strongly affected (Table 2).

The observed fast decay involves interaction between electrons and lattice phonons of the metal particles and should therefore be independent of the nanoparticle environment. But in fact, electron−phonon dependence on the environment has been reported by many researchers.[5−7] Thus, heat exchange within a thin layer of the medium around the nanoparticle dominates the fast decay component, whereas the slow component is assigned to heat conduction within the host medium.[7] In our experiment, both alkane-capped MPCs (MPC-a) and the fluorenyl-capped MPCs (MPC-b) had a similar environment near the cluster and as a result exhibited similar electron decay dynamics. However, the presence of the outer fluorene layer surrounding the alkane-capped gold particles in the 9-(9-fluorenyl)-nonane-1-thiolate MPCs (MPC-b), affected phonon−phonon interactions more than electron−phonon interactions. That is, energy transfer from the excited fluorene to the gold nanocore contributes more to the slow component than to the fast component during the electron relaxation, causing the ratio of the fast to the slow component to decrease. So the ratio of the fast component to the slow component decreased when the fluorenyl groups were present in the encapsulating layer bound to the gold clusters, whether chemically bound to the gold surface or just mixed with gold clusters. This phenomenon was observed in each MPC, irrespective of fluorenyl group content (Table 2).

Energy transfer is known to be distance-dependent. In each MPC with chemically bound fluorenyl groups (MPC-b, c, and d), energy transfer to the gold nanocore was implicated. In the optically matched solution (Match-b′, c′, and d′), only small fractions of the excited fluorene were close enough to the gold surface to exhibit efficient energy transfer. The greater the implicated energy transfer, the more of the slow component contributed to the observed decay dynamics. This explains why the ratios of the fast component to the slow component in the fluorenyl-capped MPCs (MPC-b, c, and d) were smaller than those observed in the corresponding optically matched solution.

El-sayed et al. reported that a higher fractional contribution of the slow component was observed upon 380 nm excitation than at 600 nm.[26] This difference might have been related to the higher electronic temperature T_e attained by 380 nm excitation.[26] When the fluorenyl groups were present at the periphery of the gold clusters, energy transfer produced a higher electronic temperature. An increase of the electron gas temperature led to a higher lattice temperature, which increased the relative contribution of the slow component in the gold electronic relaxation dynamics.

Thus, a bound fluorophore is a useful probe to study the ultrafast electronic relaxation dynamics. By encapsulating the metal nanoparticles with fluorophore-terminated monolayer, one can study the effect of electronic coupling between the excited fluorophore group with the metal core and hence the separate pathways for ultrafast electronic relaxation. Such experiments are very valuable in establishing the principles governing electronic relaxation in metal nanoclusters. Direct evidence of energy transfer from the fluorene to the gold electrons and the decay of the fluorene triplet−triplet absorption are still being explored.

Conclusion

Gold electronic relaxation in a series of monolayer-protected gold clusters took place through a biexponential decay with a fast electron−phonon interaction (lifetime of about 2.0 ps), followed by a slow phonon−phonon interaction (lifetime of more than 15 ps). The observed decays resembled bleached plasmon band recovery dynamics previously reported in the naked gold nanoparticles and in dodecane-1-thiolate capped gold nanoparticles.[17] Ultrafast dynamics show that the fractional coverage of **1** or **2** on the gold clusters did not change the hot electron relaxation lifetime. Instead, although energy transfer from the excited fluorene to the gold particles was not fast enough to change the observed relaxation dynamics lifetime, the ratio of the fast decay component to the slow decay component was affected by surface composition, with the contribution from the slow decay component becoming larger with larger fractional coverage by the fluorenyl substituted groups. The experiments show that the more energy transfer, the greater is the fraction of the slow decay component's contribution to decay dynamics. Residual triplet−triplet absorption in fluorophore-labeled MPCs was smaller than that in an optically matched solution of the nonane-1-thiolate MPCs and unattached **1** or **2**. This experiment also confirmed that energy transfer from bound chromophores to the gold core did take place with a rate constant k_{EN} estimated to be faster than 10^{12} s^{-1}.

Acknowledgment. This work was supported by the U.S. Department of Energy, Office of Basic Energy Science, Chemistry Division.

References and Notes

(1) Alivisatos, A. P. *J. Phys. Chem.* **1996**, *100*, 13226.
(2) Kamat, P. V. *Prog. Inorg. Chem.* **1997**, *44*, 273.
(3) Wang, Y. *Acc. Chem. Res.* **1991**, *24*, 133.
(4) (a) Link, S.; El-Sayed, M. A. *J. Phys. Chem. B* **1999**, *103*, 8410. (b) Link, S.; El-Sayed, M. A. *J. Phys. Chem. B* **1999**, *103*, 4212.
(5) Zhang, J. Z. *Acc. Chem. Res.* **1997**, *30*, 423.
(6) (a) Halte, V.; Bigot, J.-Y.; Palpant, B.; Broyer, M.; Prevel, B.; Perez, A. *Appl. Phys. Lett.* **1999**, *75*, 3799. (b) Bigot, J.-Y.; Halte, V.; Merle, J.-C.; Daunois, A. *Chem. Phys.* **2000**, *251*, 181.
(7) Link, S.; Furube, A.; Mohamed, M. B.; Asahi, T.; Masuhara, H.; El-Sayed, M. A. *J. Phys. Chem. B* **2002**, *106*, 945.
(8) (a) Gu, T.; Whitesell, J. K.; Fox, M. A., submitted for publication. (b) Cedheim, L.; Eberson, L. *Synthesis* **1973**, 159. (c) Hu, J.; Fox, M. A. *J. Org. Chem.* **1999**, *64*, 4959. (d) Hostetler, M. J.; Stokes, J. J.; Murray, R. W. *Langmuir* **1996**, *12*, 3604.
(9) Alvarez, M. M.; Khoury, J. T.; Schaaf, T. G.; Shafigullin, M. N.; Veznar, I.; Whetten, R. L.; Alvarez, M. M. *J. Phys. Chem. B* **1997**, *101*, 3706.
(10) Henglein, A. *Langmuir* **1998**, *14*, 6738.
(11) (a) Fujiwara, H.; Yanagida, S.; Kamat, P. V. *J. Phys. Chem. B* **1999**, *103*, 2589. (b) Chandrasekharan, N.; Kamat, P. V.; Hu, J.; Jones G., II. *J. Phys. Chem.* **2000**, *104*, 11103.
(12) (a) Link, S.; Burda, C.; Nikoobakht, B.; El-Sayed, M. A. *J. Phys. Chem. B* **2000**, *104*, 6152. (b) Hostetler, M. J.; Templeton, A. C.; Murray, R. W. *Langmuir* **1999**, *15*, 3782.
(13) (a) Brorson, S. D.; Fujimoto, J. G.; Ippen, E. P. *Phys. Rev. Lett.* **1987**, *59*, 1962. (b) Elsayed-Ali, H. E.; Juhasz, T.; Smith, G. O.; Bron, W. E. *Phys. Rev. B* **1991**, *43*, 19914. (c) Wright, O. B. *Phys. Rev. B* **1994**, *49*, 9985. (d) Schoenlein, R. W.; Lin, W. Z.; Fujimoto, J. G.; Eesley, G. L. *Phys. Rev. Lett.* **1987**, *58*, 1680. (e) Sun, C.-K.; Vallee, F.; Acioli, L. H.; Ippen, E. P.; Fujimoto, J. G. *Phys. Rev. B* **1994**, *50*, 15337. (f) Anisimov, L.; Kapeliovich, B. L.; Perel'man, T. L. *Sov. Phys. JETP* **1975**, *39*, 375. (g) Sun, C.-K.; Vallee, F.; Acioli, L. H.; Ippen, E. P.; Fujimoto, J. G. *Phys. Rev. B* **1993**, *48*, 12365. (h) Fann, W. S.; Storz, R.; Tom, H. W. K.; Bokor, J. *Phys. Rev. Lett.* **1992**, *68*, 2834. (i) Allen, P. B. *Phys. Rev. Lett.* **1987**, *59*, 1460. (j) Anisimov, S. I.; Kapeliovich, B. L.; Perelman, T. L. *Zh. Eksp. Teor. Fiz.* **1974**, *66*, 776 [Sov. Phys. **1975**, JETP 4, 173]
(14) Perner, M.; Bost, P.; v. Plessen, G.; Feldmann, J.; Becker, U.; Mennig, M.; Schmidt, H. *Phys. Rev. Lett.* **1997**, *78*, 2192.
(15) Perner, M.; Klar, T.; Grosse, S.; Lemmer, U.; v. Plessen, G.; Spirkl, W.; Feldmann, J. *J. Lumin.* **1998**, *76 & 77*, 181.
(16) Inouye, H.; Tanaka, K.; Tanahashi, I.; Hirao, K. *Phys. Rev. B* **1998**, *57*, 11334.
(17) Logunov, S. L.; Ahmadi, T. S.; El-Sayed, M. A.; Khoury, J. T.; Whetten, R. L. *J. Phys. Chem. B* **1997**, *101*, 3713.
(18) Ehrenreich, H.; Philipp, H. R. *Phys. Rev.* **1962**, *128*, 1622.
(19) Johnson, P. B.; Christy, R. W. *Phys. Rev. B* **1972**, *6*, 4370.
(20) Ashcroft, N. W.; Mermin, N. D. *Solid State Physics*; Harcourt Brace: Orlando, FL, 1976.
(21) Fann, W. S.; Storz, R.; Tom, H. W. K.; Bokor, J. *Phys. Rev. B* **1992**, *46*, 13592.
(22) Schmuttenmaer, C. A.; Aeschlimann, M.; Elsayed-Ali, H. E.; Miller, R. J. D.; Mantell, D. A.; Cao, J.; Gao, Y. *Phys. Rev. B* **1994**, *50*, 8957.
(23) Hertel, T.; Knoesel, E.; Wolf, M.; Ertl, G. *Phys. Rev. Lett.* **1996**, *76*, 535.
(24) Ogawa, S.; Nagano, H.; Petek, H. *Phys. Rev. B* **1997**, *55*, 10869.
(25) Knorren, R.; Bennemann, K. H.; Burgermeister, R.; Aeschlimann, M. *Phys. Rev. B* **2000**, *61*, 9427.
(26) Ahmadi, T. S.; Logunov, S. L.; El-Sayed, M. A. *J. Phys. Chem. B* **1996**, *100*, 8053.